Stereoselective Double-Helicate Assembly from Chiral 2,2′:6′,2″:6″,2‴-Quaterpyridines and Tetrahedral Metal Centres

Gerhard Baum,[b] Edwin C. Constable,*[a] Dieter Fenske,[b] Catherine E. Housecroft,[a] and Torsten Kulke[a]

Abstract: A pair of chiral 2,2′:6′,2″:6″,2‴-quaterpyridine ligands **1** and **2** have been prepared and shown to diastereoselectively assemble double-helical coordination compounds. The complexation of **1** or **2** with copper(I) or silver(I) leads to dinuclear double helicates $[M_2(L)_2]^{2+}$ with high diastereoselectivity [diastereomeric excess (*d.e.*) $\geq$ 96%] for the formation of *P* or *M* helicates. Circular dichroism (CD) studies of the helicates in solution reveal intense activity in the region of 320–328 nm that is diagnostic of *P* or *M* helical chirality. On the basis of the CD spectra it is proposed that the dominant diastereomers with **1** possess *P* helicity, whilst those with **2** possess *M* helical chirality. These proposals have been confirmed by solid-state structural determinations of the dominant diastereomers of $[Cu_2(\mathbf{1})_2][PF_6]_2 \cdot 2\,MeCN$, $[Cu_2(\mathbf{2})_2][PF_6]_2 \cdot 2\,MeCN$ and $[Ag_2(\mathbf{1})_2][PF_6]_4 \cdot 0.33\,H_2O$. Redistribution reactions of dicopper(I) and disilver(I) helicates lead to the stereoselective assembly of heterodinuclear helicates, whereas the reaction of $[Cu_2(\mathbf{1})_2]^{2+}$ with $[Cu_2(\mathbf{2})_2]^{2+}$ leads to the formation of the heterochiral, heterostranded species $[Cu_2(\mathbf{1})(\mathbf{2})]^{2+}$.

Keywords: chirality · chiral resolution · helical structures · N ligands · solid-state structures · supramolecular chemistry

Introduction

Helical coordination compounds are often prepared by self-assembly methods in which appropriate ligands react with suitable metal ions.[1–4] Helices are inherently chiral and possess a *plus* (*P*) or *minus* (*M*) handedness. Metal-directed assembly of achiral ligands to form helicates must give a racemic mixture of enantiomeric *P* and *M* helices if parity is conserved. In exceptional cases, complete or partial spontaneous resolution occurs upon crystallization of such racemates,[5, 6] but the *total* amounts of *P* and *M* helicates within the system remain constant. In order to obtain excesses of the *P* or *M* helicates, it is necessary to have an additional source of chirality in the system, such that the two are related as diastereomers rather than enantiomers. This is most readily achieved through the use of chiral ligands, and a number of examples of self-assembly processes involving such ligands have been reported.[7–18] Our initial studies with chiral 2,2′:6′,2″-terpyridine ligands demonstrated the formation of *P* or *M* helicates in reasonable diastereomeric excess when chiral substituents were incorporated in the 6- but not the 4′-position.[19–23] Double helicates formed from two tetrahedral metal centres and two 2,2′:6′,2″-terpyridine ligands are inherently unstable as a result of the incommensurate matching of donor (six nitrogen donors) and acceptor (eight coordination sites) properties. In this paper we describe an extension of these studies to the diastereoselective formation of *P* or *M* helicates from chiral 2,2′:6′,2″:6″,2‴-quaterpyridines.[24, 25]

[a] Prof. E. C. Constable, Prof. C. E. Housecroft, Dr. T. Kulke
Institut für Anorganische Chemie der Universität Basel
Spitalstrasse 51, CH-4056 Basel (Switzerland)
Fax: (+41) 61-267-1015
E-mail: constable@ubaclu.unibas.ch

[b] Prof. D. Fenske, G. Baum
Institut für Anorganische Chemie der Universität Karlsruhe
Engesserstrasse, Geb.:30.45, D-76128, Karlsruhe (Germany)

Results and Discussion

2,2′:6′,2″:6″,2‴-Quaterpyridine helicates and ligand design: The ligand 2,2′:6′,2″:6″,2‴-quaterpyridine (qtpy) may be partitioned into two didentate 2,2′-bipyridine metal-binding domains and has been shown to form dinuclear double helicates with metal ions that favour a tetrahedral coordination geometry, such as copper(I) or silver(I).[26–29] It has also been shown that the introduction of substituents into the 6 position of 2,2′-bipyridine metal-binding domains results in the stabilization of tetrahedral over octahedral coordination geometries.[30–33]

Von Zelewsky and co-workers have shown that pinene-based chirality can be easily combined with 2,2′-bipyridine

  0947-6539/99/0506-1862 $ 17.50+.50/0

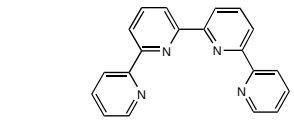

qtpy

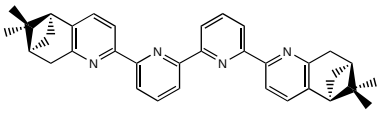

1

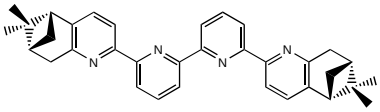

2

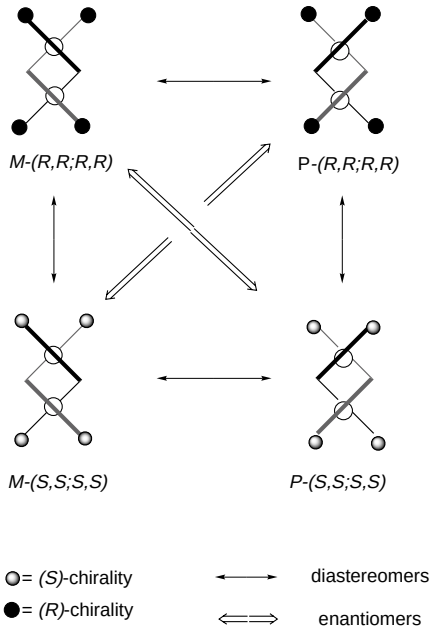

Figure 1. The introduction of chiral substituents into a helicand results in the formation of diastereomeric double helicates. Inversion of all chirality ($M \leftrightarrow P$, $R \leftrightarrow S$) gives the enantiomeric pairs of compounds {(*P*)-(*R*,*R*;*R*,*R*) and (*M*)-(*S*,*S*;*S*,*S*)} and {(*P*)-(*S*,*S*;*S*,*S*) and (*M*)-(*R*,*R*;*R*,*R*)}. All other combinations of compounds are related as diastereomers.

metal-binding domains, and that such ligands undergo stereoselective complexation reactions with transition metal ions[34, 35] and may be used as enantioselective building blocks in metallosupramolecular chemistry.[11, 36, 37] More recently, copper(I) complexes with pinene-functionalized 1,10-phenanthroline complexes have also been shown to be formed stereoselectively.[38] The great advantage of the pinene-based systems is the stability of the chiral auxiliary—it is extremely unlikely that subsequent manipulation of the system will result in racemization of the auxiliary. In order to maximize chiral induction and to eliminate additional complexity from the formation of head-to-head (*HH*) or head-to-tail (*HT*) isomers,[39] we decided to prepare the bifunctionalized C_2 symmetrical chiral ligands **1** and **2**.

A double helix possesses an inherent clockwise or anticlockwise helicity. The chirality is determined from the view along the principal helical axis: a clockwise motion corresponds to a *P* and an anticlockwise motion to an *M* helix. Achiral ligands yield a racemic mixture of *P* and *M* helicates, and separation by chromatographic methods with chiral supports or mobile phases is not viable when labile metal centres are involved. In order to selectively form *P* or *M* helicates it is necessary to include additional stereochemical information in the system. With chiral ligands, the *P* and *M* helicates are related as diastereomers. In contrast to enantiomers, diastereomers have different chemical and physical properties and will not necessarily be formed in equal amounts. A homochiral ligand containing two chiral auxiliaries can exist as a pair of *S*,*S* or *R*,*R* enantiomers; if the functionality is symmetrically disposed, no *HH* or *HT* isomers are formed, and a total of four homoleptic double helicates (Figure 1) are possible. Of these, the (*P*)-(*R*,*R*;*R*,*R*) and (*M*)-(*R*,*R*;*R*,*R*) helicates are diastereomers, as are the (*P*)-(*S*,*S*;*S*,*S*) and (*M*)-(*S*,*S*;*S*,*S*) pair. In contrast, the (*P*)-(*R*,*R*;*R*,*R*) and (*M*)-(*S*,*S*;*S*,*S*) helicates are related as enantiomers, as are the (*P*)-(*S*,*S*;*S*,*S*) and (*M*)-(*R*,*R*;*R*,*R*) pair. Thus, if an enantiomerically pure ligand is taken, a pair of diastereomeric (*P*)-(*S**,*S**;*S**,*S**) and (*M*)-(*S**,*S**;*S**,*S**) helicates will be formed. Any chiral induction will be expressed as an excess of the *P* or *M* helicate. With labile metal centres, the system is expected to reach thermodynamic equilibrium between the *P* or *M* helicates and, assuming that no interconversion of *ligand* chirality occurs, the measured diastereomeric excess (*d.e.*) depends only on the free-energy difference between the two helicates.

The use of a racemic mixture of ligands containing both the *S*,*S* and *R*,*R* enantiomers would lead to additional isomeric possibilities. In addition to the homoleptic helicates discussed above, the heteroleptic pair of helicates (*P*)-(*S*,*S*;*R*,*R*) and (*M*)-(*R*,*R*;*S*,*S*) could be produced. These are related as a pair of enantiomers, although the *S*,*S* and *R*,*R* ligands are chemically (and magnetically) different in each case. With the specific system chosen, in which each ligand possesses two centres of chirality, there is also the possibility of a third, achiral, *meso* isomer of the ligand, in which each ligand bears one *R* and one *S* chiral centre. This *R*,*S* ligand will not be discussed further, but we note that in this case, the *P* and *M* helicates are now related as enantiomers, and that *HH* and *HT* isomers are also possible.

Preparation of the chiral 2,2′:6′,2″:6″,2‴-quaterpyridines 1 and 2: The synthetic approach adopted is presented in Scheme 1 and is based upon the Kröhnke pyridine synthesis.[40] The activated 6,6′-diacetyl-2,2′-bipyridine derivative **3** is the key intermediate for the chiral quaterpyridines **1** and **2**, and is obtained directly from the reaction of 6,6′-diacetyl-2,2′-bipyridine with iodine and pyridine.[41] The enone chosen for reaction with **3** determines the chirality and substitution

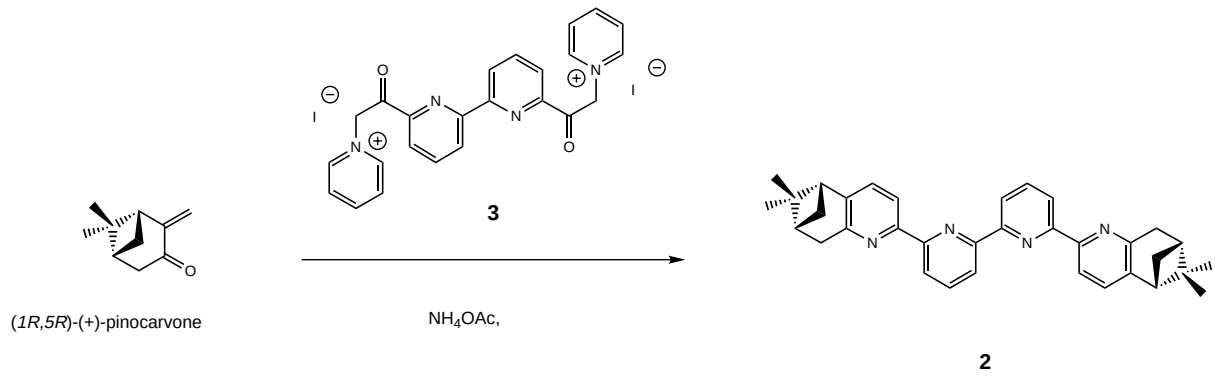

Scheme 1. Preparation of chiral quaterpyridines.

pattern in the final oligopyridine, and the use of (+)- or (−)-pinocarvones produces the desired 5,6;5‴6‴-disubstituted ligands.

The reaction of freshly prepared **3** with (1*R*,5*R*)-(+)-pinocarvone under an inert atmosphere in the presence of an excess of $[NH_4][OAc]$ proceeded smoothly in boiling glacial acetic acid containing 10% acetic anhydride to give compound **2**. The enantiomer (all-*S*)-**1** was prepared in a similar manner from (1*S*,5*S*)-(−)-pinocarvone. Other solvents were found to be less effective and it appears to be crucial that freshly prepared **3** is used. The new ligands (all-*S*)-**1** and (all-*R*)-**2** were obtained as microanalytically pure, white solids in over 80% yield after recrystallization from ethanol.

The time-of-flight (TOF) mass spectra of **1** and **2** showed molecular-ion peaks at $m/z = 499$ together with peaks assigned to sodium and potassium adducts. The ^{1}H NMR spectra (Tables 1, 2) were well-resolved and fully assigned by chemical shift comparison and NOE-difference spectroscopy. Further discussion of the spectra is reserved until later.

Table 1. ^{1}H NMR spectroscopic data (250 MHz) for the aromatic resonances of $CDCl_3$ solutions of the ligand **1** and CD_3CN solutions of the complexes $[Ag_2(\mathbf{1})_2][PF_6]_2$ and $[Cu_2(\mathbf{1})_2][PF_6]_2$. Data are only given for the major diastereomer of each complex. The spectra of **2** and the complexes $[Ag_2(\mathbf{2})_2][PF_6]_2$ and $[Cu_2(\mathbf{2})_2][PF_6]_2$ are identical to those of their enantiomers within experimental error.

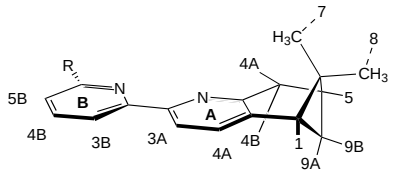

	3A/δ	4A/δ	3B/δ	4B/δ	5B/δ
1	8.31 d	7.38 d	8.42 dd	7.94 t	8.62 dd
$[Ag_2(\mathbf{1})_2][PF_6]_2$	7.66 d	7.47 d	8.06 d	7.96 t	7.74 d
$[Cu_2(\mathbf{1})_2][PF_6]_2$	7.87 d	7.56 d	7.89 dd	7.67 t	7.46 dd

The chiral ligands were also studied by polarimetry and CD spectroscopy. The optical rotations (Na-D line) were of the same magnitude but opposite in sign (Table 3). The recrystallized ligands possess an enantiomeric purity similar to, or better than, that of the starting pinacarvones and the CD

Table 3. Compilation of the free ligand and complex rotational values and CD signal intensities. The $[\alpha]_D$ and $[M]_D$ values come from polarimetric measurements and the $\Delta\varepsilon$ values from CD spectroscopy. All data for the free ligands **1** and **2** are for $CHCl_3$ solutions, whilst those for the complexes refer to CH_3CN solutions.

	$[\alpha]_D$ [° g^{-1} cm^3 dm^{-1}]	$[M]_D$ [° cm^3 dm^{-1} mol^{-1}] [a]	$\Delta\varepsilon_{max}$ [mol^{-1} l cm^{-1}]
1	+66.8[b]	+333[b]	$\Delta\varepsilon_{269}$ +4.6[c]
2	−67.0[b]	−334[b]	$\Delta\varepsilon_{269}$ −4.4[c]
P-$[Ag_2(\mathbf{1})_2]^{2+}$	+1 128[d]	+16 950[d]	$\Delta\varepsilon_{320}$ +273[e]
M-$[Ag_2(\mathbf{2})_2]^{2+}$	−1 132[d]	−17 012[d]	$\Delta\varepsilon_{320}$ −276[e]
P-$[Cu_2(\mathbf{1})_2]^{2+}$	+2 126[d]	+30 068[d]	$\Delta\varepsilon_{328}$ +341[e]
M-$[Cu_2(\mathbf{2})_2]^{2+}$	−2 138[d]	−30 237[d]	$\Delta\varepsilon_{328}$ −346[e]

[a] $[M]_D = [\alpha]_D \times MW/100$. [b] $c = 0.63$ g cm^{-3}. [c] Concentrations of **1** and **2**, 3.81×10^{-4} and 4.71×10^{-4} mol l^{-1}, respectively. [d] Concentrations of $[Ag_2(\mathbf{1})_2]^{2+}$, $[Ag_2(\mathbf{2})_2]^{2+}$, $[Cu_2(\mathbf{1})_2]^{2+}$ and $[Cu_2(\mathbf{2})_2]^{2+}$ were 0.166, 0.128, 0.0285 and 0.0282 g cm^{-3}, respectively. [e] Concentrations of $[Ag_2(\mathbf{1})_2]^{2+}$, $[Ag_2(\mathbf{2})_2]^{2+}$, $[Cu_2(\mathbf{1})_2]^{2+}$ and $[Cu_2(\mathbf{2})_2]^{2+}$ were 3.22×10^{-4}, 3.03×10^{-4}, 2.01×10^{-4} and 1.63×10^{-4} mol l^{-1}, respectively.

responses are, within experimental error, equal and opposite for **1** and **2**; signal intensities were lower than $\Delta\varepsilon \pm 5$ mol^{-1} l cm^{-1} with a maximum absorption difference at 269 nm and weaker signals at 301 nm with $\Delta\varepsilon \pm 1.4$ mol^{-1} l cm^{-1}. These correspond to maxima at 265 and 300 nm, assigned to $n-\pi^*$ or $\pi-\pi^*$ transitions in the electronic absorption spectrum.

Synthesis of metal complexes: The complexes $[Ag_2(L)_2][PF_6]_2$ (L = **1** or **2**) were prepared by ultrasonication of an equimolar mixture of silver(I) acetate and the appropriate ligand in MeOH followed by precipitation of the $[PF_6]^-$ salts. Deep red solutions of the copper(I) complexes were obtained from the

Table 2. ^{1}H NMR spectroscopic data (250 MHz) for the aliphatic resonances of $CDCl_3$ solutions of the ligand **1** and CD_3CN solutions of the complexes $[Ag_2(\mathbf{1})_2][PF_6]_2$ and $[Cu_2(\mathbf{1})_2][PF_6]_2$. Data are only given for the major diastereomer of each complex. The spectra of **2** and the complexes $[Ag_2(\mathbf{2})_2][PF_6]_2$ and $[Cu_2(\mathbf{2})_2][PF_6]_2$ are identical to those of their enantiomers within experimental error.

	H1/δ	H4A/δ	H4B/δ	H5/δ	H7/δ	H8/δ	H9A/δ	H9B/δ
1	2.83 t	3.21 d	3.21 d	2.41 m	0.69 s	1.43 s	1.33 d	2.72 m
$[Ag_2(\mathbf{1})_2][PF_6]_2$	2.85 t	2.63 dd	1.65 dd	1.94 m	0.36 s	1.30 s	0.98 d	2.66 m
$[Cu_2(\mathbf{1})_2][PF_6]_2$	2.90 t	2.35 dd	2.23 dd	2.00 m	0.37 s	1.30 s	1.24 d	2.69 m

0947-6539/99/0506-1864 $ 17.50+.50/0 *Chem. Eur. J.* **1999**, *5*, No. 6

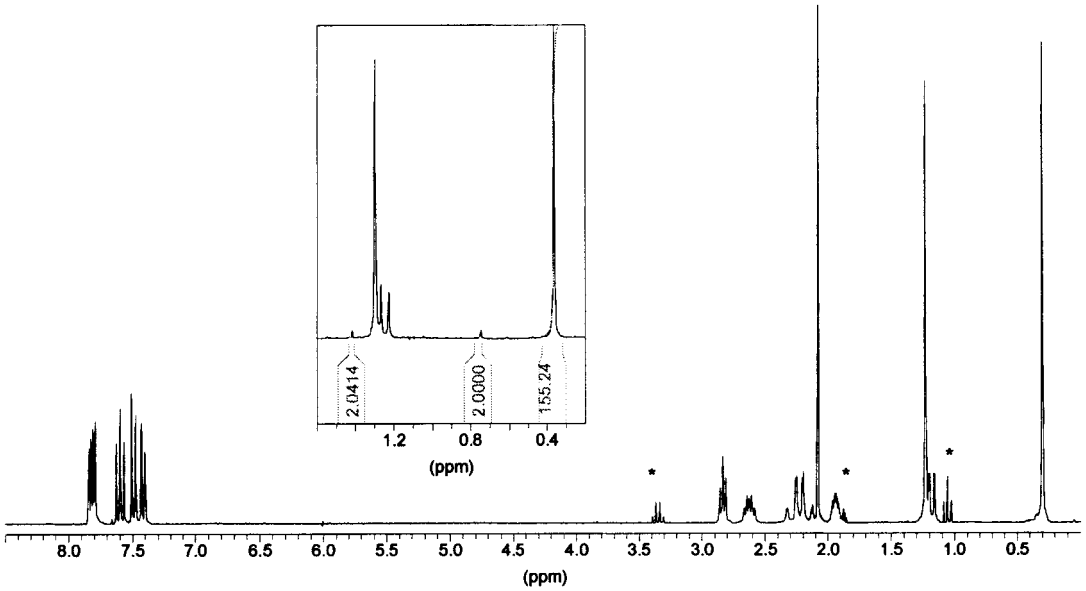

Figure 2. ^{1}H NMR spectrum (250 MHz, CD_3CN) of the diastereomerically pure complex $[Cu_2(\mathbf{1})_2][PF_6]_2$ as obtained after a single recrystallization. The peaks marked with an asterisk arise from residual NMR solvent or the diethyl ether used in the recrystallization. The inset displays a part of the spectrum of the crude complex with the integral values showing the 2:155 ratio of diastereomeric complexes obtained initially.

reaction of $[Cu(MeCN)_4][PF_6]$ and **1** or **2** by ultrasonication of deaereated MeCN solutions. In all cases, the crude products consisted of a mixture of major and minor diastereomers, but slow diffusion of diethyl ether into the MeCN solutions gave microanalytically pure, single diastereomers of $[M_2(L)_2][PF_6]_2$. The presence of the substituents in the 6-position results in high oxygen stability for the copper(I) complexes; solutions of $[Cu_2(L)_2]^{2+}$ in MeCN (10^{-4} M) are unchanged after exposure to air for one year.

Yields of the crude complexes were in excess of 95 % and no polymeric or other side-products were observed by tlc analysis of the reaction mixtures. The chiral auxiliary confers high solubilities on the complexes in halogenated solvents and typically 15 mg of complex may be dissolved in 0.5 mL of CH_2Cl_2. The TOF mass spectra of the complexes support the dinuclear formulation and exhibit $[M - PF_6]^+$ peaks at $m/z =$ 1269 and 1358 for $[Cu_2(L)_2][PF_6]_2$ and $[Ag_2(L)_2][PF_6]_2$, respectively.

^{1}H NMR spectroscopic studies: The metal complexes are diamagnetic and their ^{1}H NMR spectra are well-resolved and so provide a convenient method of assessing the diastereoselectivity of helicate formation. The ^{1}H NMR spectra of CD_3CN solutions of the *crude* precipitates consisted of a major (> 97.5 %) and a minor set of resonances, (Figures 2, 3). The spectra of the complexes obtained with **1** and **2** were identical. The ratio of diastereomers is best seen by considering the singlet assigned to H^{9A} (inset, Figure 2). The two species in solution are the diastereomeric *P* and *M* helicates. If the major resonances correspond to the *P* helicate with **1**, then

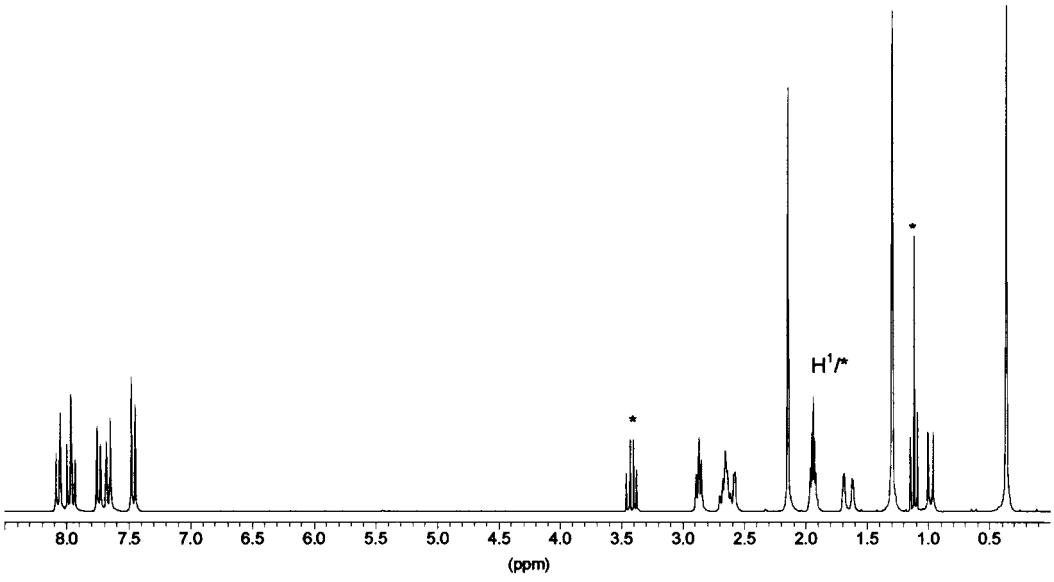

Figure 3. ^{1}H NMR spectrum (250 MHz, CD_3CN) of the diastereomerically pure complex $[Ag_2(\mathbf{2})_2][PF_6]_2$ as obtained from a single recrystallization. The peaks marked with an asterisk arise from residual NMR solvent or the diethyl ether used in the recrystallization.

they correspond to the enantiomeric *M* helicate with **2** and vice versa. The ^{1}H NMR spectra of the recrystallized materials showed only the resonances of the major diastereomer and confirmed the expected D_2 helicate symmetry (Tables 1, 2). The ^{1}H NMR results suggest that a high degree of stereoselectivity has been attained. However, a level of caution is necessary before this conclusion can be reached.

Whilst there is no doubt that the major and minor signals correspond to the *P* and *M* helicates, the phenomenon has two possible origins. The first is that chiral induction is high and a given ligand produces an excess of the *P* or *M* diastereomers. The second is that the starting ligands were not enantiomerically pure, and as **1** and **2** are enantiomers NMR spectroscopy will not reveal the presence of the opposite enantiomer. The starting pinacarvones are more than 99% enantiomerically pure, but always contain some of the opposite enantiomer. The result is that, for example, in the preparation of **1**, the majority of the ligand will possess *S*,*S* chirality, but some *meso* *R*,*S* compound and a very small amount of **2** will also have been formed. Unless these chiral impurities have been eliminated during work-up, they will be present in the ligand used for complexation and will be expressed in the various diastereomeric helicates.

We have now unambiguously established that the first explanation is correct. Both dicopper(I) and disilver(I) double helicates are labile and ligand redistribution reactions occur over a period of hours to days. As noted earlier, recrystallization of the mixture of diastereomers gave only the major species. Solutions of the recrystallized single diastereomers slowly regenerate the minor subspectrum. Re-equilibration takes around 2 days at ambient temperature and restores the original signal intensities observed in the crude, nonrecrystallized products. As the ligand chirality is frozen, the formation of the mixture of diastereomers establishes that an equilibrium between the *P* and *M* species does exist, and that the ratios originally observed reflect the relative stabilty of the two species and that the complexation methodology leads to thermodynamic equilibrium. Accordingly, it is meaningful to discuss the ratios of the major and minor species in detail.

After re-equilibration the major and minor species in solutions of $[Cu_2(L)_2][PF_6]_2$ were present in ratios of 155:2, which corresponds to a *d.e.* of 98.7%, $\ln K = 4.35$ and ΔG (298 K) $= -10.8$ kJ mol^{-1}. The diastereoselectivity is less for the silver complexes $[Ag_2(L)_2][PF_6]_2$ and the two components are present in re-equilibrated solutions in a ratio of 42:1 (*d.e.* = 96.3%, $\ln K = 3.73$ and ΔG (298 K) $= -9.3$ kJ mol^{-1}). A number of resonances undergo significant changes upon coordination and give important information regarding intramolecular interactions. In general, the resonances of the aromatic protons are shifted upfield, of which H^{5B} is close to the interannular C–C bond between the two bpy domains of a given ligand and is expected to be especially sensitive to conformational change. The largest coordination shifts observed are the upfield shifts of H^{5B} by $\Delta\delta = 0.88$ in the silver complexes and by $\Delta\delta = 1.16$ in the copper complexes. In the aliphatic region, H^{4A} and H^{4B} are diastereotopic, but are isochronous in the free ligand even though the protons are in remarkably different environments, as has previously been noted in related pinene-substituted pyridines.[34] This degeneracy is removed in the helicates and the protons are separated by $\delta = 0.2 - 1.0$; inter alia, this reveals the ^2J geminal coupling constants of 18–21 Hz. Such an increase in magnetic degeneracy upon coordination does not appear to be have observed previously. The silver complexes generally show a more pronounced shift difference between H^{4A} and H^{4B} than the copper helicates. Unambiguous assignment of H^{4A} and H^{4B} was possible through a weak NOE contact between H^7 and H^{4A}. The NOE experiments also disclosed that H^{4A} exhibits a partially resolved, long-distance coupling that results in a broadening of the doublet, an effect not observed with H^{4B}. The pinene H^7 and H^8 protons are sensitive to *P* or *M* helical chirality; the major component of $[Cu_2(L)_2][PF_6]_2$ exhibits singlets at $\delta = 0.37$ (H^7) and 1.30 (H^8), whilst the corresponding resonances of the minor diastereomer are at $\delta = 0.75$ (H^7) and 1.42 (H^8). This indicates that the ligands in the two diastereomers are in distinctly different environments. On the basis of the ^{1}H NMR spectroscopic data alone we are unable to say whether the major diastereomers possess *P* or *M* helical chirality.

Re-equilibration experiments: Before addressing the question of the conformation of the major and minor diastereomers, some other aspects of the dynamic behaviour of these systems will be discussed. The lability of the helicates has been established above and allows some interesting exchange experiments to be carried out. In a first experiment, equimolar amounts of $[Cu_2(\mathbf{1})_2]^{2+}$ and $[Cu_2(\mathbf{2})_2]^{2+}$ salts were mixed and allowed to equilibrate in solution in MeCN. This experiment was expected to give rise to three NMR observable species; the major and minor diastereomers of the homoleptic helicates and also a new heteroleptic $[Cu_2(\mathbf{1})(\mathbf{2})]^{2+}$ compound. The homoleptic species would only give rise to two subspectra, because (*P*)-$[Cu_2(\mathbf{1})_2]^{2+}$ and (*M*)-$[Cu_2(\mathbf{2})_2]^{2+}$ are enantiomers, as are (*P*)-$[Cu_2(\mathbf{2})_2]^{2+}$ and (*M*)-$[Cu_2(\mathbf{1})_2]^{2+}$. The ^{1}H NMR spectrum of the mixture shows, after equilibration, a 155:20:2 mixture of compounds (Scheme 2). The new component is the C_2-symmetrical, heterostranded, heterochiral $[Cu_2(\mathbf{1})(\mathbf{2})]^{2+}$ helicate and the ratio of 155:20 corresponds to $\ln K = 2.05$, ΔG (298 K) $= -5.07$ kJ mol^{-1}. This heterostranded compound is remarkable in that each ligand is homochiral, but that the two ligands in the complex are enantiomers. Thus, their net chirality cancels and the only net chirality arises from the *P* or *M* helicity. The (*P*)- or (*M*)-$[Cu_2(\mathbf{1})(\mathbf{2})]^{2+}$ helicates are enantiomers and are formed in equal amounts, but give rise to two sets of NMR signals because the two ligands are *chemically* and *magnetically independent*. No separation has been attempted because of the low amounts formed and the kinetic lability of $[Cu_2(\mathbf{1})(\mathbf{2})]^{2+}$. A related experiment has been independently reported by Stack.[42]

In a second experiment, we considered the formation of heterometallic helicates, which we have previously described in the 2,2′:6′,2″:6″,2‴:6‴,2⁗-quinquepyridine series.[43–45] Equimolar amounts of $[Cu_2(\mathbf{1})_2]^{2+}$ and $[Ag_2(\mathbf{1})_2]^{2+}$ salts were mixed and equilibrated in MeCN solution. This is expected to form a reaction mixture of the major and minor diastereomers of the starting complexes together with a pair of diastereomers corresponding to (*P*)- and (*M*)-$[CuAg(\mathbf{1})_2]^{2+}$ heteronu-

0947-6539/99/0506-1866 $ 17.50+.50/0 *Chem. Eur. J.* **1999**, *5*, No. 6

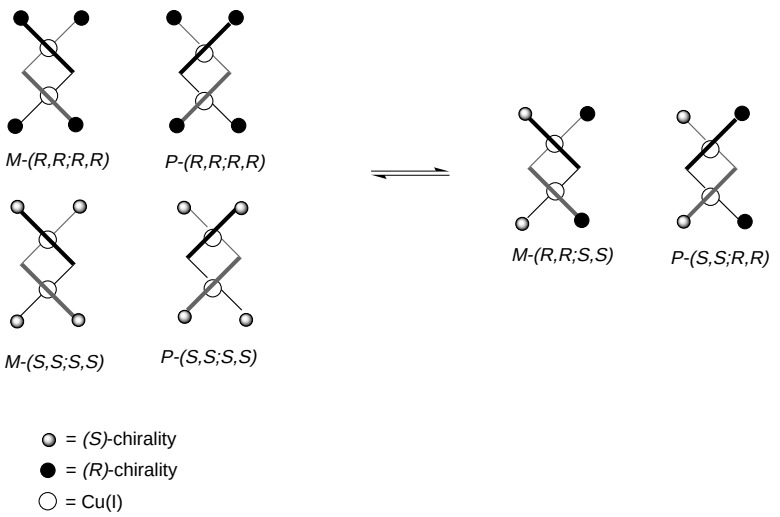

Scheme 2. Stereochemical outcome of re-equilibration experiments with $[Cu_2(\mathbf{1})_2]^{2+}$ and $[Cu_2(\mathbf{2})_2]^{2+}$.

clear species (Scheme 3). To simplify the discussion only the major solution species will be considered—that is to say the *major* diastereomers of each complex. Assuming that the two starting complexes possess the same helicity (vide infra), a heterometallic, homostranded, homochiral $[AgCu(\mathbf{1})_2]^{2+}$ helicate of the same helicity as the starting complexes is expected after equilibration. Equilibration is relatively fast and 80% complete after 90 min. After 2 days the ratio of the major component subspectra was 7:2:7 for the $[Cu_2(\mathbf{1})_2]^{2+}$:$[AgCu(\mathbf{1})_2]^{2+}$:$[Ag_2(\mathbf{1})_2]^{2+}$ components (Figure 4, p. 1868). The heterodinuclear $[AgCu(\mathbf{1})_2]^{2+}$ helicate has a lower symmetry than its homometallic congeners, and in the ^{1}H NMR spectrum a C_2 rather than a D_2 symmetrical species is observed. It is interesting to note that a statistical 1:2:1 mixture is not formed, although, according to Le Chatelier's principle, addition of $[Ag_2(\mathbf{1})_2]^{2+}$ shifts the equilibrium towards $[AgCu(\mathbf{1})_2]^{2+}$ at the expense of the $[Cu_2(\mathbf{1})_2]^{2+}$ complex.

X-Ray structure determinations: The identity of the helical chirality of the major and minor diastereomers was established by a combination of solid-state structural determination and solution-phase circular dichroism (CD) spectroscopy. The crystal and molecular structures of the major diastereomers of $[Cu_2(\mathbf{1})_2][PF_6]_2\cdot 2\,MeCN$, $[Cu_2(\mathbf{2})_2][PF_6]_2\cdot 2\,MeCN$ and $[Ag_2(\mathbf{1})_2][PF_6]_2\cdot 0.33\,H_2O$ were solved; crystals were obtained in each case by the slow diffusion of diethyl ether vapour into MeCN solutions and were shown by ^{1}H NMR spectroscopy to consist of the pure major diastereomer. Crystal data for the three determinations are presented in Table 4.

Solid-state structures of $[Cu_2(\mathbf{1})_2][PF_6]_2\cdot 2\,MeCN$ and $[Cu_2(\mathbf{2})_2][PF_6]_2\cdot 2\,MeCN$: Both structures were solved in the noncentrosymmetric orthorhombic space group $P2_12_12_1$ and are identical within experimental error. The solid-state structures of the $[Cu_2(\mathbf{1})_2]^{2+}$ cation are presented in Figure 5 (p. 1869) and confirm the double-helical geometry and that the major diastereomer of $[Cu_2(\mathbf{1})_2]^{2+}$ exhibits *P* helical chirality. The $[Cu_2(\mathbf{2})_2]^{2+}$ cation exhibted *M* chirality. The Flack parameters[46] are close to zero in each case, establishing the absolute structures. The double-helical nature of the complexes is clearly seen in the space-filling representation of the $[Cu_2(\mathbf{1})_2]^{2+}$ cation in Figure 5b. The bond angles and distances are within the typical range of similar $[Cu_2(qtpy)_2]^{2+}$ cations.[28–31] The Cu–N distances (2.018(3)–2.102(4) Å) are unremarkable, although the Cu···Cu distances within the individual cations of 3.414 and 3.419 Å are slightly longer than observed in some other dicopper(I) qtpy complexes (3.17, 3.32 Å)[28–31]—an observation attributed to the larger steric demands of the 5,6-substituted ligands. The helication is achieved by a twist between the central rings of each ligand (39.9–43.3°), although smaller twists are also observed at the outer rings (15.9–20.5°). Intrastrand π-stacking between terminal and central pyridine rings (3.8–3.9 Å) is also observed and might stabilize further the helical architecture.

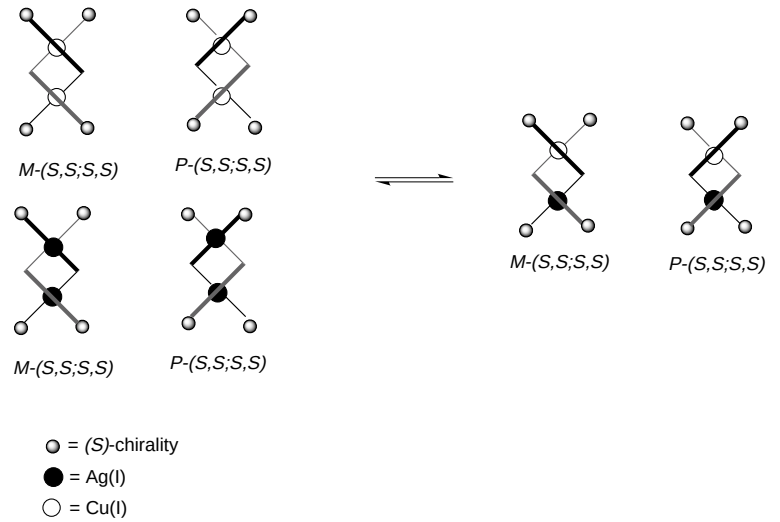

Scheme 3. Stereochemical outcome of re-equilibration experiments with $[Cu_2(\mathbf{1})_2]^{2+}$ and $[Ag_2(\mathbf{1})_2]^{2+}$

Solid-state structure of $[Ag_2(\mathbf{1})_2][PF_6]_2\cdot 0.33\,H_2O$: This structure was solved in the noncentrosymmetric cubic space group $F432$. The solid-state structure confirmed the double-helical structure (Figure 6a, p. 1870) and a helical *P* conformation (best seen in the space-filling representation in Fig-

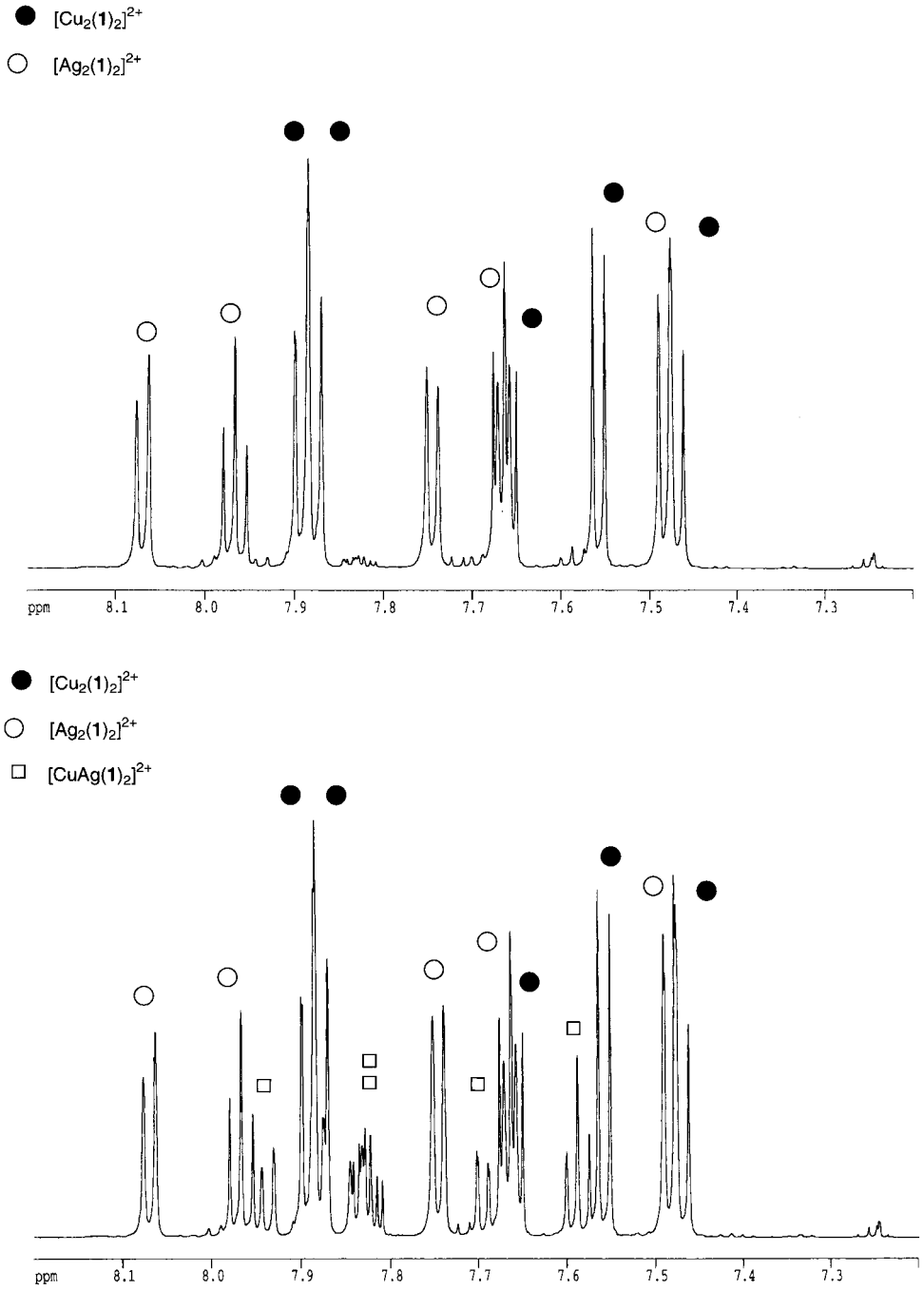

Figure 4. Comparison of the aromatic regions of the ^{1}H NMR spectra (600 MHz, CD_3CN) of a 1:1 mixture of $[Cu_2(\mathbf{1})_2][PF_6]_2$ and $[Ag_2(\mathbf{1})_2][PF_6]_2$: a) after 6 min, predominantly the homometallic copper(I) and silver(I) complexes, and b) after 18 h when equilibrium has been reached. The additional signals correspond to the newly formed heterometallic complex of the major diastereomer, which possesses the same *P* helicity as the starting materials.

ure 6b). The Flack parameters confirmed the absolute structural assignment. The Ag–N distances (2.245(6), 2.343(6) Å) closely resemble those in the parent $[Ag_2(qtpy)_2]^{2+}$ complex (2.223 – 2.409 Å).[29, 31] The Ag···Ag distance of 3.230(2) Å is longer than observed in $[Ag_2(qtpy)_2]^{2+}$ (3.107(2) Å)[29, 31] as a result of pinene-ligand repulsion. As with the copper complexes, the principal twisting occurs between the two central rings (41.4°) although a significant twist of 17.4° occurs at the outer rings. Once again, intrastrand π-stacking between terminal and central pyridine rings (3.7 – 3.9 Å) is observed.

A comparison of the complexes shows that the different intermetallic (Cu···Cu, 3.414, 3.419 Å; Ag···Ag, 3.230 Å) and metal – nitrogen distances (Cu–N, 2.018 – 2.102 Å; Ag–N, 2.245 – 2.343 Å) combine to change the pitch of the helix. The Ag···Ag distance is shorter than the Cu···Cu distance, even though the silver cation ($r = 1.14$ Å) is considerably larger than the copper cation ($r = 0.74$ Å). Each metal is in a distorted tetrahedral arrangement and the metal – ligand interactions are expressed in bite angles of 81.3 – 82.0° in the dicopper(I) and 73.0° in the disilver(I) complexes. The decreased angles in the latter complex reflect the longer Ag–N distances.

Origins of diastereoselectivity: The solid-state structural determinations allow a detailed analysis of the origin of the diastereoselectivity. We had expected the diastereoselectivity to arise from interactions between pineno substituents of the two ligand strands. In the structures of (*P*)-$[Cu_2(\mathbf{1})_2]^{2+}$ and (*M*)-$[Cu_2(\mathbf{2})_2]^{2+}$ the closest contacts across the helicate between adjacent pinene methyl groups are 5.0 Å (shortest H···H) and 6.3 Å (shortest C···C). Although the chiral centres are in closer proximity than in complexes we have prepared previously,[19, 20] the high level of diastereoselectivity cannot be accounted for by these long-range contacts. The bridging methylene group of the four-membered pinene ring is, however, very close to a central pyridine ring of the other qtpy helicand and the shortest contacts are 2.65 Å (shortest H···H) and 4.3 Å (shortest C···C; see Figure 7a, p. 1870). This short distance explains why the pitch is elongated compared with previously published structures.[29–31] If the helical pitch were decreased, then the pinene methylene group would experience severe steric interactions with pyridine rings of the other ligand. ^{1}H NMR spectroscopic studies in solution support this explanation and H^{9A} is shifted upfield in the complexes compared with the free ligand. In the helicate, H^{9A} lies above a pyridine ring of the other ligand and is in the

0947-6539/99/0506-1868 $ 17.50+.50/0 *Chem. Eur. J.* **1999**, *5*, No. 6

Table 4. Crystal data, data collection, and refinement parameters.[a]

	$[Cu_2(\mathbf{1})_2][PF_6]_2 \cdot 2MeCN$	$[Cu_2(\mathbf{2})_2][PF_6]_2 \cdot 2MeCN$	$[Ag_2(\mathbf{1})_2][PF_6]_2 \cdot 0.33H_2O$
formula	$C_{72}H_{74}Cu_2F_{12}N_{10}P_2$	$C_{72}H_{74}Cu_2F_{12}N_{10}P_2$	$C_{68}H_{68.66}Ag_2F_{12}N_8O_{0.33}P_2$
M_r	1496.43	1496.43	1502.27
colour, habit	red-brown needles	red-brown needles	pale yellow icosahedra
lattice type	orthorhombic	orthorhombic	cubic
space group	$P2_1\,2_1\,2_1$	$P2_1\,2_1\,2_1$	$F\,4\,3\,2$
a [Å]	14.881(2)	14.902(4)	36.654(4)
b [Å]	20.572(2)	20.494(3)	36.654(4)
c [Å]	22.435(3)	22.391(3)	36.654(4))
V [Å^3]	6868.1(15)	6838.2(23)	49 245 (93)
Z	4	4	24
ρ_{calcd} [g cm^{-3}]	1.447	1.454	1.216
F (000)	3088	3088	18256
radiation used	$Mo_{K\alpha}$	$Mo_{K\alpha}$	$Mo_{K\alpha}$
μ [mm^{-1}]	0.749	0.753	0.582
θ range [°]	2.27–26.05	2.41–25.59	1.84–25.10
unique reflections measured	13160	12075	3672
unique reflections observed, $I > 2\sigma[I]$	10081	9487	2577
parameters	855	855	225
restraints	0	0	13
R	0.0492	0.0592	0.0743
w$R2$	0.1126	0.1517	0.2169
R (all data)	0.0712	0.0772	0.0956
w$R2$ (all data)	0.1234	0.1646	0.2403
Weighting factors, a,b[b]	0.0599, 2.0811	0.0999, 3.2614	0.1724, 0.00
Absolute structure parameter	0.005(12)	−0.02(2)	0.01(9)
largest difference peak, hole [e Å^{-3}]	0.389, −0.310	0.788, −0.511	2.619, −0.481

[a] Details in common: graphite monochromated radiation, Stoe IPDS diffractometer, 200 K, refinement based on F^2. [b] $w^{-1} = [\sigma^2(F_o^2) + (aP)^2 + bP]$ where $P = (F_o^2 + 2F_c^2)/3$

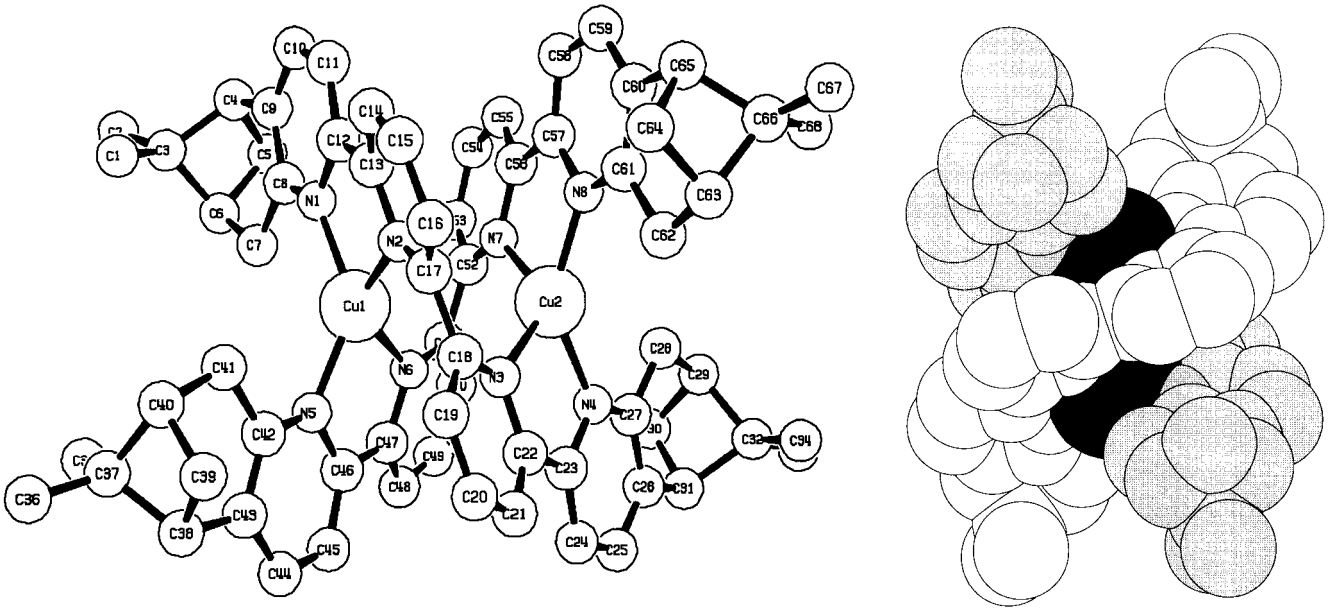

a) b)

Figure 5. Crystal and molecular structure of a) the double-helical cation in the lattice of (*P*)-$[Cu_2(\mathbf{1})_2][PF_6]_2 \cdot 2MeCN$ showing the numbering scheme; H atoms have been omitted for clarity, and b) a space-filling representation with the ligands shaded to emphasize the double-helical nature.

shielding region generated by the magnetic anisotropy of the aromatic ring. The upfield shift for H^{9A} depends on the pitch and differs in the copper ($\Delta\delta = 0.09$) and silver ($\Delta\delta = 0.40$) complexes. More interestingly, the methyl protons H^7 and H^8, which show no significant intrahelical interactions, are found at virtually identical shifts in the silver and copper complexes.

Exchange of the CH_2 and $C(CH_3)_2$ groups in the complexes inverts the ligand chirality but maintains the helical chirality. The energetically disfavoured (*P*)-$[Cu_2(\mathbf{2})_2]^{2+}$ helicate may be

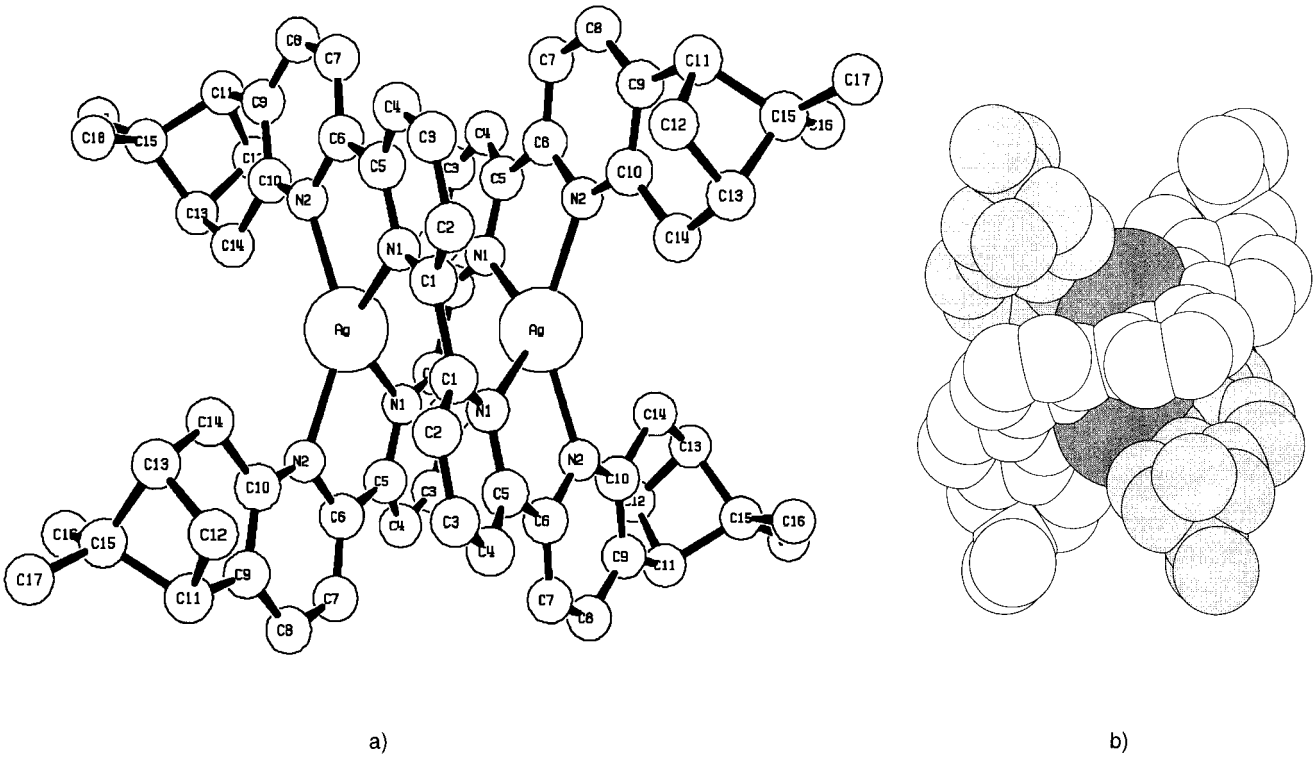

Figure 6. Crystal and molecular structure of a) the double-helical cation in the lattice of (*P*)-$[Ag_2(\mathbf{1})_2][PF_6]_2 \cdot 2MeCN$ showing the numbering scheme; H atoms have been omitted for clarity, and b) a space-filling representation with the ligands shaded to emphasize the double-helical nature.

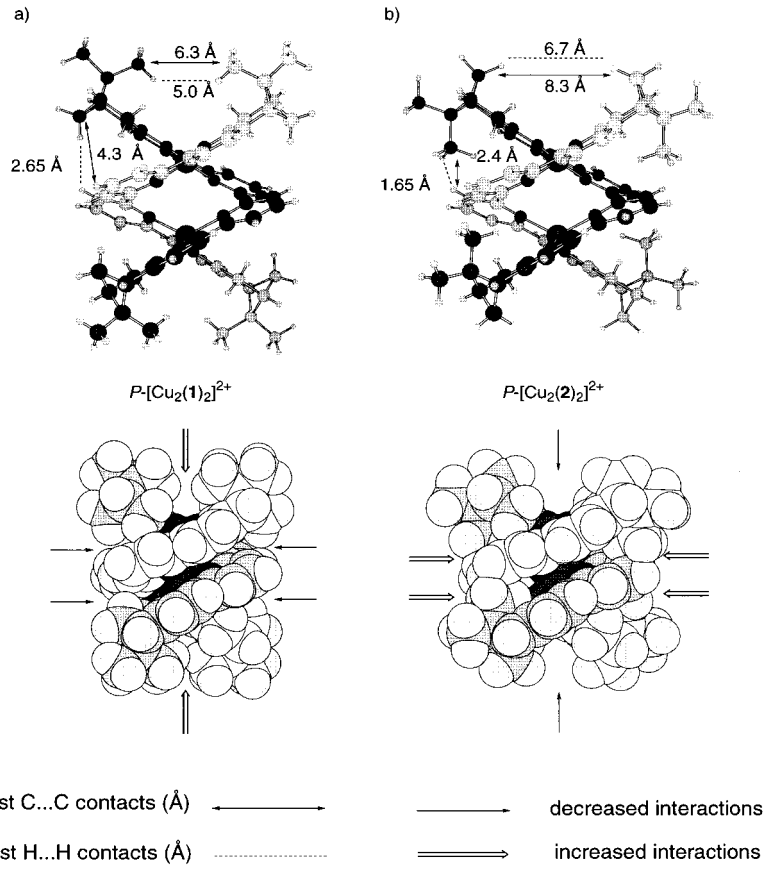

Figure 7. a) The double-helical cation in the lattice of (*P*)-$[Cu_2(\mathbf{1})_2][PF_6]_2 \cdot 2MeCN$ showing close contacts, and b) the modelled structure of a (*P*)-$[Cu_2(\mathbf{2})_2]^{2+}$ cation showing the increased steric interactions between the ligands.

modelled on the solid-state (*P*)-$[Cu_2(\mathbf{1})_2]^{2+}$ cation with no other changes made to the structure.[47] In this structure, the closest distance *between* adjacent pinene groups is increased to 6.7 Å (shortest H···H) and 8.3 Å (shortest C···C). However, the pinene $C(CH_3)_2$ groups would approach the central pyridine rings of the other helicand to give contacts of 1.65 Å (shortest H···H) and 2.4 Å (shortest C···C). The increase in pitch necessary to alleviate these interactions results in a weakening of the M–N interactions and an overall destabilization. Identical arguments apply to the silver complexes.

It is now apparent that the diastereoselectivity arises from interligand pinene – pyridine interactions and *not* from the initially anticipated interactions *between* two pinene substituents. This also explains why only a 155:20:2 ratio of compounds has been obtained upon equilibration of $[Cu_2(\mathbf{1})_2]^{2+}$ and $[Cu_2(\mathbf{2})_2]^{2+}$. The formation of

0947-6539/99/0506-1870 $ 17.50+.50/0 *Chem. Eur. J.* **1999**, *5*, No. 6

the heterostranded, heterochiral $[Cu_2(\mathbf{1})(\mathbf{2})]^{2+}$ helicate is disfavoured because one ligand, regardless of the overall *P* or *M* helicity, will have lower steric interactions (corresponding to the energetically favoured isomer, Figure 7a), whereas the other ligand must have the increased interactions of the energetically disfavoured isomer (Figure 7b).

Chirooptical properties: Finally, we can consider the chirooptical properties of these complexes and correlate these with the ligand and helical chirality. For consistency, equilibrated solutions of the complexes, containing the equilibrium distribution of *P* and *M* helicates, were studied. In each case, the CD spectra of the complexes for a given metal were equal and opposite (Figure 8), providing direct experimental evidence for the formation of enantiomeric (*P*)-$[M_2\{(S)\text{-}L\}_2]$ and (*M*)-$[M_2\{(R)\text{-}L\}_2]$ or (*M*)-$[M_2\{(S)\text{-}L\}_2]$ and (*P*)-$[M_2\{(R)\text{-}L\}_2]$ helicates. All complexes show strong activity at 320–328 nm as well as weaker signals towards shorter wavelengths (Table 3). The copper(I) complexes display additional weak bands at 457 nm with the same sign as the signal at 320–328 nm and approximately coincident with an MLCT band. The 320–328 nm CD responses are considerably more intense than for the free ligand. Combining the observations from CD and ^{1}H NMR spectroscopy, we can state that the helicates maintain their structural integrity in solution.

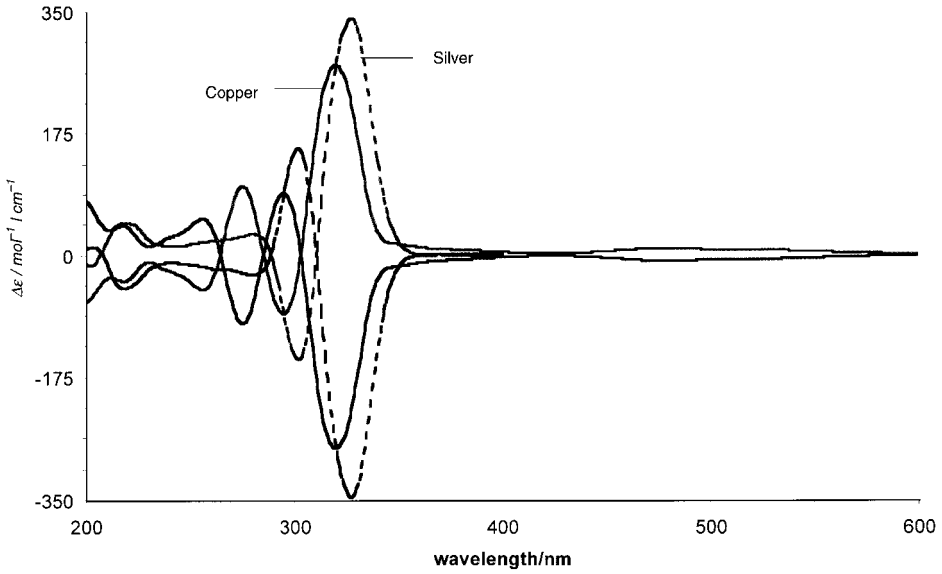

Figure 8. Circular dichroism spectra of equilibrated MeCN solutions of the complexes containing as the major diastereomer (*P*)-$[Cu_2(\mathbf{1})_2][PF_6]_2$, (*M*)-$[Cu_2(\mathbf{2})_2][PF_6]_2$, (*P*)-$[Ag_2(\mathbf{1})_2][PF_6]_2$ and (*M*)-$[Ag_2(\mathbf{2})_2][PF_6]_2$. In each case, the *P* diastereomer shows positive values of $\Delta\varepsilon$.

As with the free ligands, the signals at 320–328 nm correspond primarily to ligand-centred $\pi-\pi^*$ transitions. The enhancement of these CD responses arises from exciton coupling,[48] and it has been suggested that the sign may be used to determine the absolute configuration at the metal centres and hence to assign overall *P* or *M* helicity. On the basis of theoretical models and model compounds it is proposed that a positive absorption is characteristic of a *P* helicate and a negative absorption of a *M* helicate.[48] Accordingly, the solution CD spectra indicate the formation of (*P*)-$[Ag_2(\mathbf{1})_2]^{2+}$, (*M*)-$[Ag_2(\mathbf{2})_2]^{2+}$, (*P*)-$[Cu_2(\mathbf{1})_2]^{2+}$ and (*M*)-$[Cu_2(\mathbf{2})_2]^{2+}$, fully in accord with the solid-state studies. We concur completely with the proposals regarding the assignment of absolute configuration of helicates from CD spectra and are confident that for oligopyridine-based helicates the method may be used when solid-state data are not available.

The optical rotations of the various compounds have also been determined by polarimetry. The complexes possess the same absolute sense of rotation as the free ligands, but have significantly larger values (Table 3). The use of the molar rotations leads us to make an interesting aside. According to the van't Hoff additivity principle the molar rotation can be divided into two components, one from the ligand and one from the double helix, as there are no significant absorptions at 589 nm. Thus, subtraction of twice the ligand molar rotational values from the values for the complexes will approximate to the residual rotations from the double helix. In the case of the copper complex, the double helix contributes $\pm 31\,200^\circ\,cm^3\,dm^{-1}\,mol^{-1}$, whereas in the case of the silver complex a helical molar rotation of $-16\,300^\circ\,cm^3\,dm^{-1}\,mol^{-1}$ is calculated. In other words, 96–98% of the entire optical rotation can be attributed to the helix. The differences between the silver and copper complexes parallel those observed in related knotted systems, in which the molar value for the copper complex is roughly double that of the silver.[49]

Conclusions

The stereoselective self-assembly of double helicates in high diastereomeric excess from chiral oligopyridines has been demonstrated. Redistribution reactions of dicopper(I) and disilver(I) helicates lead to the stereoselective assembly of heterodinuclear helicates. The stereoselectivity arises from interactions between the chiral auxiliaries and the oligopyridine strands. Chirooptical studies suggest that the helix, and not the ligand chirality, is the major contributor to the molar ellipticity, and also that the CD responses and optical rotations are sensitive to changes in helical pitch. The high molar rotations and molar absorption coefficient differences are expected to increase further in longer helicates and in systems in which topological contributions are added to the Euclidean chirality of the double helix. We are currently incorporating such helical chirality as a structural component in novel supramolecular assemblies.

Experimental Section

General methods: IR spectra were recorded on a Mattson Genesis FT spectrophotometer with samples in pressed KBr discs. ^{1}H NMR spectra were recorded on a Bruker AM 250 or Avance 600 spectrometer. UV/Vis measurements were performed with a Perkin – Elmer Lambda 19 spectrophotometer. Optical rotations were measured on a Perkin – Elmer 141 polarimeter at the Na-D line in 10 cm quartz cuvettes. CD spectra were recorded with a Jasco J-720 CD spectrometer in 1 mm quartz cuvettes at 25 °C. Time-of-flight (MALDI) spectra were recorded on a PerSeptive Biosystems Voyager-RP Biospectrometry Workstation. The compounds 6,6′-bis-(1-pyridinioacetyl)-2,2′-bipyridine **3**,[41] (1*R*)-(+)- and (1*S*)-(−)-pinocarvone[50] were prepared following published procedures. The starting pinene chiralities were of highest commercially available purity (*e.e.* ≥ 98 %).

5,6:5‴,6‴-Bis-[(1*S*,5*S*)-(+)-pineno]-2,2′:6′,2″:6″,2‴-quaterpyridine (1): A mixture of freshly prepared **3** (0.325 g, 0.5 mmol), (1*S*)-(−)-pinocarvone (0.18 g, 1.2 mmol) and ammonium acetate (0.7 g, 9 mmol) was refluxed under an inert atmosphere in glacial acetic acid (5 mL) and acetic anhydride (0.5 mL) for 16 h, during which period a cream solid was precipitated. The reaction mixture was poured into a mixture (1:1, 20 mL) of aqueous NaOH (2 M) and MeOH, and the precipitate collected by filtration, dissolved in CH_2Cl_2 and then filtered through Celite. The filtrate was concentrated in vacuo and recrystallized from EtOH (50 mL) to give white crystals of **1** (0.21 g, 84 %). M.p. > 250 °C; ^{13}C NMR (75 MHz, $CDCl_3$, 25 °C, TMS): $\delta = 21.35, 26.09, 31.98, 36.74, 39.58, 40.29, 46.54, 117.97, 120.40, 120.64, 133.75, 137.61, 142.27, 153.71, 155.46, 155.88, 156.35$; IR (KBr): $\tilde{\nu} =$ 2919 (s), 1563 (s), 1431 (s), 1421 (s), 807 cm^{-1} (s); MS (MALDI, TOF): *m*/*z*: 499 $[M]^+$; UV/Vis ($CDCl_3$, 5.72×10^{-4} M): λ_{max} (ε_{max}) = 265 (26.2×10^3), 300 nm (42.9×10^3); $C_{34}H_{34}N_4$ (498.3): calcd C 81.9, H 6.9, N 11.2; found C 81.5, H 6.9, N 11.2.

5,6:5‴,6‴-Bis-[(1*R*,5*R*)-(−)-pineno]-2,2′:6′,2″:6″,2‴-quaterpyridine (2): Compound **2** was prepared analogously to **1** from **3** (0.325 g, 0.5 mmol) and (1*R*)-(+)-pinocarvone (0.18 g, 1.2 mmol); it was isolated as white crystals (0.20 g, 81 %). M.p. > 250 °C. UV/Vis ($CDCl_3$, 5.72×10^{-4} M): λ_{max} (ε_{max}) = 265 (26.2×10^3), 300 nm (42.6×10^3); $C_{34}H_{34}N_4$ (498.3): calcd C 81.9, H 6.9, N 11.2; found C 81.9, H 7.1, N 11.2.

General method for preparation of the complexes: A solution of AgOAc (16.7 mg, 0.1 mmol) in MeOH (5 mL) or of $[Cu(MeCN)_4][PF_6]$ (37.5 mg, 0.1 mmol) in degassed MeCN (2 mL) was treated with the appropriate ligand (49.9 mg, 0.1 mmol) and the mixture was then ultrasonicated for 5 – 10 min at RT. Any remaining solids were removed by filtration through Celite after which aqueous $[NH_4][PF_6]$ was added. The resultant precipitate was collected by filtration, washed with water, dried (P_2O_5) and recrystallized by slow diffusion of diethyl ether into an acetonitrile solution.

$[Cu_2(1)_2][PF_6]_2$: Red needles (71 mg, 100 %); IR (KBr): $\tilde{\nu} = 2933$ (s), 1589 (m), 1561 (s), 1433 (s), 1422 (m), 1245 (m), 839 (s), 557 cm^{-1} (s); MS (MALDI, TOF): *m*/*z*: 1269 $[M - PF_6]^+$, 1124 $[M - 2PF_6]^+$, 562 $[Cu(\mathbf{1})]^+$, 499 $[\mathbf{1}]^+$; UV/Vis (MeCN, 3.54×10^{-4} M): λ_{max} (ε_{max}) = 272 (58.6×10^3), 311 nm (53.5×10^3), 457 nm (0.78×10^3); $C_{68}H_{68}F_{12}N_8P_2Cu_2$ (1412.3): calcd C 57.75, H 4.85, N 7.9; found C 57.4; H 4.7; N 8.1.

$[Cu_2(2)_2][PF_6]_2$: Red needles (71 mg, 100 %); IR (KBr): $\tilde{\nu} = 2933$ (s), 1589 (m), 1564 (s), 1436 (s), 1419 (m), 1247 (m), 841 (s), 557 cm^{-1} (s); MS (MALDI, TOF): *m*/*z*: 1269 $[M - PF_6]^+$, 1124 $[M - 2PF_6]^+$, 562 $[Cu(\mathbf{2})]^+$, 499 $[\mathbf{2}]^+$; UV/Vis (MeCN, 1.63×10^{-4} M): λ_{max} (ε_{max}) = 272 (58.5×10^3), 311 (53.5×10^3), 457 nm (0.82×10^3); $C_{68}H_{68}F_{12}N_8P_2Cu_2$ (1412.3): calcd C 57.75, H 4.85, N 7.9; found C 57.7; H 4.8; N 8.2.

$[Ag_2(1)_2][PF_6]_2$: Pale yellow crystals (72 mg, 96 %); IR (KBr): $\tilde{\nu} = 2926$ (s), 1564 (s), 1431 (s), 1422 (s), 1264 (w), 833 (s), 560 cm^{-1} (s); MS (MALDI, TOF): *m*/*z*: 1358 $[M - PF_6]^+$, 1105 $[M - 2PF_6 - Ag]^+$, 606 $[Ag(\mathbf{1})]^+$, 499 $[\mathbf{1}]^+$; UV/Vis (MeCN, 3.22×10^{-4} M): λ_{max} (ε_{max}) = 264 (42.1×10^3), 307 nm (43.9×10^3); $C_{68}H_{68}F_{12}N_8P_2Ag_2 \cdot H_2O$ (1518.3): calcd C 53.7, H 4.6, N 7.4; found C 53.3; H 4.6; N 7.4.

$[Ag_2(2)_2][PF_6]_2$: Pale yellow crystals (73 mg, 97 %); IR (KBr): $\tilde{\nu} = 2924$ (s), 1562 (s), 1432 (s), 1422 (s), 1264 (w), 833 (s), 560 cm^{-1} (s); MS (MALDI, TOF): *m*/*z* 1358 $[M - PF_6]^+$, 1105 $[M - 2PF_6 - Ag]^+$, 606 $[Ag(\mathbf{1})]^+$, 499 $[\mathbf{1}]^+$; UV/Vis (MeCN, 3.03×10^{-4} M): λ_{max} (ε_{max}) = 264 (41.8×10^3), 307 nm (43.6×10^3); $C_{68}H_{68}F_{12}N_8P_2Ag_2 \cdot H_2O$ (1518.3): calcd C 53.7, H 4.6, N 7.4; found C 53.7; H 4.5; N 7.3.

X-ray crystallography: Table 4 provides a summary of the crystal data, data collection, and refinement parameters for the three crystal structures reported in this paper. The structures were solved by direct methods with SHELXS-86 and refined with SHELXL-93[51, 52] by full matrix least-squares based on F^2. The non-hydrogen atoms were refined anisotropically while the hydrogen atoms were placed in idealized positions and assigned isotropic thermal parameters. Compounds $[Cu_2(\mathbf{1})_2][PF_6]_2 \cdot 2MeCN$ and $[Cu_2(\mathbf{2})_2][PF_6]_2 \cdot 2MeCN$ represent the two enantiomers of this molecule and their unit cell parameters only differ within experimental error. The structure of $[Cu_2(\mathbf{2})_2][PF_6]_2 \cdot 2MeCN$ was refined by inverting all coordinates of $[Cu_2(\mathbf{1})_2][PF_6]_2 \cdot 2MeCN$. In all cases, Friedel pairs were measured to enable refinement of the Flack parameter, which converged at 0.005(12) for $[Cu_2(\mathbf{1})_2][PF_6]_2 \cdot 2MeCN$, −0.02(2) for $[Cu_2(\mathbf{2})_2][PF_6]_2 \cdot 2MeCN$, and 0.01(9) for $[Ag_2(\mathbf{1})_2][PF_6]_2 \cdot 0.33H_2O$ to confirm the absolute configurations. Crystallographic data (excluding structure factors) for the structures reported in this paper have been deposited with the Cambridge Crystallographic Data Center as supplementary publication no. CCDC-100885 ($[Cu_2(L)_2][PF_6]_2 \cdot 2MeCN$) and as Refcode ROJTAL ($[Ag_2(\mathbf{1})_2][PF_6]_2 \cdot 0.33H_2O$). Copies of the data can be obtained free of charge on application to CCDC, 12 Union Road, Cambridge CB2 1EZ, UK (fax: (+44) 1223-336-033; e-mail: deposit@ccdc.cam.ac.uk).

Acknowledgments

We thank the Schweizerischer Nationalfonds zur Förderung der wissenschaftlichen Forschung and the University of Basel for financial support of this work. We also thank Professors Alexander von Zelewsky and Jean-Pierre Sauvage for helpful discussions and provision of unpublished material.

[1] E. C. Constable, *Tetrahedron*, **1992**, *48*, 10013.
[2] E. C. Constable, *Prog. Inorg. Chem.* **1994**, *42*, 67.
[3] E. C. Constable, in *Comprehensive Supramolecular Chemistry*, *Vol. 9* (Ed.: J.-M. Lehn), Pergamon, Oxford, **1996**, pp. 213.
[4] C. Piguet, G. Bernardinelli, G. Hopfgartner, *Chem. Rev.* **1997**, *97*, 2005.
[5] R. Krämer, J.-M. Lehn, A. DeCian, J. Fischer, *Angew. Chem.* **1993**, *105*, 764; *Angew. Chem. Int. Ed. Engl.* **1993**, *32*, 703.
[6] P. N. Baxter, J.-M. Lehn, K. Rissanen, *Chem. Commun.* **1997**, 1323.
[7] W. Zarges, J. Hall, J.-M. Lehn, C. Bolm, *Helv. Chim. Acta* **1991**, *74*, 1843.
[8] C. R. Woods, M. Benaglia, F. Cozzi, J. S. Siegel, *Angew. Chem.* **1996**, *108*, 1977; *Angew. Chem. Int. Ed. Engl.* **1996**, *35*, 1830.
[9] A. L. Airey, G. F. Swiegers, A. C. Willis, S. B. Wild, *Inorg. Chem.* **1997**, *36*, 1588.
[10] C. Provent, S. Hewage, G. Brand, G. Bernardinelli, L. J. Charbonniere, A. F. Williams, *Angew. Chem.* **1997**, *109*, 1346; *Angew. Chem. Int. Ed. Engl.* **1997**, *36*, 1287.
[11] O. Mamula, A. von Zelewsky, G. Bernadinelli, *Angew. Chem.* **1998**, *110*, 301; *Angew. Chem. Int. Ed.* **1998**, *37*, 289.
[12] H. Mürner, G. Hopfgartner, A. von Zelewsky, *Inorg. Chim. Acta* **1998**, *271*, 36.
[13] J. W. Canary, C. S. Allen, J. M. Castagnetto, Y. Wang, *J. Am. Chem. Soc.* **1995**, *115*, 8484.
[14] C. R. Woods, M. Benaglia, P. Blom, A. Fuchicello, F. Cozzi, J. S. Siegel, *Polym. Prep.* **1996**, *37*, 480.
[15] C. R. Woods, M. Benaglia, F. Cozzi, J. S. Siegel, *Angew. Chem.* **1996**, *108*, 1977; *Angew. Chem. Int. Ed. Engl.* **1996**, *35*, 1830.
[16] G. C. van Stein, G. van Koten, C. Brevard, *J. Organomet. Chem.* **1982**, *226*, 27.
[17] G. C. van Stein, G. van Koten, B. de Bok, L. C. Taylor, K. Vrieze, *Inorg. Chim. Acta* **1984**, *89*, 29.
[18] G. C. van Stein, G. van Koten, K. Vrieze, C. Brevard, A. L. Spek, *J. Am. Chem.* Soc. **1984**, *106*, 4486.
[19] E. C. Constable, T. Kulke, M. Neuburger, M. Zehnder, *New J. Chem.* **1997**, *21*, 633.
[20] E. C. Constable, T. Kulke, M. Neuburger, M. Zehnder, *New J. Chem.* **1997**, *21*, 1091.

0947-6539/99/0506-1872 $ 17.50+.50/0 *Chem. Eur. J.* **1999**, *5*, No. 6

[22] E. C. Constable, T. Kulke, M. Neuburger, M. Zehnder, *Chem. Commun.* **1997**, 489.
[23] G. Baum, E. C. Constable, D. Fenske, C. E. Housecroft, T. Kulke, *Chem. Commun*. **1998**, 2659.
[24] G. Baum, E. C. Constable, D. Fenske, T Kulke, *Inorg. Chem. Commun.* **1998**, *1*, 80.
[25] G. Baum, E. C. Constable, D. Fenske, T Kulke, *Chem. Commun.* **1997**, 2043.
[26] J.-M. Lehn, J.-P. Sauvage, J. Simon, R. Ziessel, C. Piccinni-Leopardi, G. Germain, J.-P. Declercq, M. Van Meerssche, *Nouv. J. Chim.* **1983**, *7*, 413.
[27] E. C. Constable, M. J. Hannon, A. Martin, P. R. Raithby, D. A Tocher, *Polyhedron* **1992**, *11*, 2967.
[28] K. T. Potts, M. Keshavarz-K, F. S. Tham, H. D. Abruña, C. R. Arana, *Inorg. Chem.* **1993**, *32*, 4422.
[29] E. C. Constable, S. M. Elder, M. J. Hannon, A. Martin, P. R. Raithby, D. A. Tocher, *J. Chem. Soc. Dalton Trans.* **1996**, 2423.
[30] R. Krämer, J.-M. Lehn, A. Marquis-Rigault, *Proc. Nat. Acad. Sci.* **1993**, *90*, 5394.
[31] A. F. Williams, *Chem. Eur. J.* **1997**, *3*, 15.
[32] W. W. Brandt, F. P. Dwyer, E. C. Gyarfas, *Chem. Rev.* **1954**, *54*, 959.
[33] W. R. McWhinnie, J. D. Miller, *Adv. Inorg. Chem. Radiochem.* **1969**, *12*, 135.
[34] P. Hayoz, A. von Zelewsky, *Tetrahedron Lett.* **1992**, *33*, 5165.
[35] P. Hayoz, A. von Zelewsky, H. Stoeckli-Evans, *J. Am. Chem. Soc.* **1993**, *115*, 5111.
[36] P. Belser, S. Bernhard, E. Jandrasics, A. von Zelewsky, L. de Cola, V. Balzani, *Coord. Chem. Rev.* **1997**, *159*, 1.
[37] N. C. Fletcher, F. R. Keene, H. Viebrock, A. von Zelewsky, *Inorg. Chem.* **1997**, *36*, 1113.
[38] E. Riesgo, A. Credi, L. de Cola, R. P. Thummel, *Inorg. Chem.* **1998**, *37*, 2145.
[39] E. C. Constable, F. Heirtzler, M. Neuburger, M. Zehnder, *J. Am. Chem. Soc.* **1997**, *119*, 5606.
[40] F. Kröhnke, *Synthesis* **1976**, 1.
[41] E. C. Constable, M. D. Ward, D. A. Tocher, *J. Chem. Soc. Dalton Trans.* **1991**, 1675.
[42] M. A. Masood, E. J. Enemark, T. D. P. Stack, *Angew. Chem.* **1998**, *110*, 973; *Angew. Chem. Int. Ed.* **1998**, *37*, 928.
[43] E. C. Constable, J. V. Walker, *J. Chem. Soc. Chem. Commun.* **1992**, 884.
[44] E. C. Constable, A. J. Edwards, P. R. Raithby, J. V. Walker, *Angew. Chem.* **1993**, *105*, 1486; *Angew. Chem. Int. Ed. Engl.* **1993**, *32*, 1465.
[45] E. C. Constable, A. J. Edwards, P. R. Raithby, D. Smith, J. V. Walker, L. A. Whall, *Chem. Commun.* **1996**, 2551.
[46] H. D. Flack, *Acta Crystallogr. Sect. A* **1983**, *39*, 876.
[47] Modelling studies used the crystallographic coordinates of the (*P*)-$[Cu_2(\mathbf{1})_2]^{2+}$ cation as a starting point. Manipulations were made with Chem3D Pro or Molecular Simulations Cerius$^{2\,TM}$ software.
[48] M. Ziegler, A. von Zelewsky, *Coord. Chem. Rev.*, in press.
[49] J.-P. Sauvage, personal communication.
[50] E. D. Mihelich, D. J. Eickhoff, *J. Org. Chem.* **1983**, *48*, 4135.
[51] G. M. Sheldrick, *SHELXS-86 Program for the Solution of Crystal Structures*, University of Göttingen, Germany, **1986**.
[52] G. M. Sheldrick, *SHELXL-93 Program for the Refinement of Crystal Structures*, University of Göttingen, Germany, **1993**.

Received: November 16, 1998 [F1442]